Functional characterization of a ClC transporter by solid-supported membrane electrophysiology

Juan Garcia-Celma, Adrian Szydelko, and Raimund Dutzler

Department of Biochemistry, University of Zürich, CH-8057 Zürich, Switzerland

EcClC, a prokaryotic member of the ClC family of chloride channels and transporters, works as coupled H^+/Cl^- exchanger. With a known structure and the possibility of investigating its behavior with different biochemical and biophysical techniques, the protein has become an important model system for the family. Although many aspects of its function have been previously characterized, it was difficult to measure transport on the same sample under different environmental conditions. To overcome this experimental limitation, we have studied EcClC by solid-supported membrane electrophysiology. The large transport-related transient currents and a simple way of relating transport rates to the measured signal have allowed a thorough investigation of ion selectivity, inhibition, and the dependence of transport on changes in ion concentration and pH. Our results confirm that the protein transports larger anions with about similar rates, whereas the smaller fluoride is not a substrate. We also show that 4,4′-diisothiocyano-2,2'-stilbenedisulfonic acid (DIDS), a known inhibitor of other anion transport protein, irreversibly inhibits EcClC from the intracellular side. The chloride dependence shows an apparent saturation at millimolar concentrations that resembles a similar behavior in eukaryotic ClC channels. Our experiments have also allowed us to quantify the pH dependence of transport. EcClC shows a strong activation at low pH with an apparent pKa of 4.6. The pronounced pH dependence is lost by the mutation of a conserved glutamate facing the extracellular solution that was previously shown to be an acceptor for transported protons, whereas it is largely retained by the mutation of an equivalent residue at the intracellular side. Our results have provided a quantitative basis for the transport behavior of EcClC, and they will serve as a reference for future investigations of novel electrogenic transporters with still-uncharacterized properties.

The Journal of General Physiology

INTRODUCTION

The ClC proteins constitute a large family of chloride transport proteins that are ubiquitously expressed in pro- and eukaryotic organisms. These membrane proteins show an unusual functional breadth, as some of them work as passive ion channels, which catalyze the selective flow of chloride down its electrochemical gradient, whereas others are secondary active transporters that couple the stoichiometric exchange of chloride to the movement of protons in the opposite direction (Miller, 2006; Accardi and Picollo, 2010). Despite these functional differences, both branches share very similar molecular architectures (Dutzler, 2007; Feng et al., 2010; Jayaram et al., 2011). In humans, the family consists of nine different members with strictly divided functional properties. Four ClC proteins expressed at the plasma membrane of different cells (ClC-1, ClC-2, ClC-Ka, and ClC-Kb) function as gated ion channels, and five family members in intracellular organelles (ClC 3–7) function as chloride-proton exchangers (Zifarelli and Pusch, 2007; Graves et al., 2008; Jentsch, 2008).

The prokaryotic ClC transporter EcClC (or ClC-ec1), a close homologue of the family expressed in the bacterium *Escherichia coli*, is a prototypic Cl^-/H^+ exchanger (Accardi and Miller, 2004). Its crystal structure has provided a molecular framework for the family and revealed the structural basis for anion selectivity (Dutzler et al., 2002). The protein is homodimeric, with each subunit containing an independent ion transport path. Chloride is bound to three consecutive sites located at the constriction of an hourglass-shaped ion translocation path (Dutzler et al., 2003; Lobet and Dutzler, 2006). In the EcClC structure, the ion binding site facing the extracellular solution is occupied by a conserved glutamate residue (Glu148 or Glu_{ex}), which controls the entrance and exit of chloride to the binding region in both channels and transporters and which additionally plays a central role in proton transport (Dutzler et al., 2003; Accardi and Miller, 2004). Besides its importance for structural studies, EcClC has also become a model system for mechanistic investigations of H^+/Cl^- exchange. Reversal potential measurements of EcClC in planar lipid bilayers have allowed the discovery of secondary active transport within a family, which was previously believed to solely consist of ion channels (Accardi and

Correspondence to Raimund Dutzler: dutzler@bioc.uzh.ch

Abbreviations used in this paper: DIDS, 4,4′-diisothiocyano-2,2'-stilbenedisulfonic acid; LPR, lipid-to-protein ratio; SSM, solid-supported membrane.

The Rockefeller University Press $30.00
J. Gen. Physiol. Vol. 141 No. 4 479–491
www.jgp.org/cgi/doi/10.1085/jgp.201210927

Miller, 2004). In WT proteins, a strict 2 Cl^- to 1 H^+ exchange stoichiometry is observed, whereas the tight coupling breaks down in mutants of Cl^- coordinating residues (Accardi et al., 2006; Walden et al., 2007). Similar measurements allowed for the identification of the residues serving as the entry sites for transmembrane proton transport on both sides of the membranes. Glu_{ex}, the extracellular H^+ acceptor, is located at one of the chloride binding sites, whereas the intracellular H^+ acceptor Glu203 (or Glu_{in}) is remote from the binding region, thus suggesting that both ions share a common path on the extracellular end that diverges at the intracellular side (Accardi and Miller, 2004; Accardi et al., 2005). The measurement of transport rates by electrochemical methods (Walden et al., 2007) and the investigation of chloride binding by x-ray crystallography and calorimetry (Lobet and Dutzler, 2006; Picollo et al., 2009, 2012) reinforce the unusual transport mode in ClC proteins, which differs from common alternate access mechanisms of secondary active transporters.

Despite the thorough investigation by different biochemical and biophysical techniques, it was challenging to quantify transport in response to changes in ion composition, substrate concentration, and pH on the same sample. To overcome these experimental limitations, we have studied EcClC-mediated ion transport into liposomes by solid-supported membrane (SSM) electrophysiology (Schulz et al., 2008). These recordings show robust transport-mediated transient currents, which are proportional to the turnover of the transporter and which allow the detailed characterization of its transport properties. Although overall in agreement with previous measurements, our results provide novel insight into the pH and ion dependence of transport through EcClC with high accuracy.

MATERIALS AND METHODS

Protein preparation

Mutants of EcClC were prepared with the QuikChange site-directed mutagenesis kit (Agilent Technologies) and verified by DNA sequencing. WT protein and mutants were expressed and purified in the detergent *n*-decyl-β-D-maltoside (DM), as described previously (Dutzler et al., 2002), with the following modifications: (1) the protein was expressed in a BL21(DE3)-derived *E. coli* strain that was reported to contain lower amounts of outer membrane porins (Accardi et al., 2004); and (2) the Superdex-200 size-exclusion step was substituted by cation-exchange chromatography on POROS 50HS cation exchange resin (Applied Biosystems).

Reconstitution into liposomes

E. coli total lipid extract (Avanti Polar Lipids, Inc.) dissolved in chloroform was dried under N_2 and resuspended in reconstitution buffer (100 mM potassium phosphate and 25 mM citrate adjusted with KOH to pH 7.6) to a final concentration of 10 mg/ml. For reconstitution of vesicles containing chloride, 30 mM KCl was added to the reconstitution buffer. The suspension was sonicated to homogeneity and extruded 21 times thorough a 400-nm filter with a LipoSofast-Basic extruder (Avestin). Liposomes were aliquoted, frozen in liquid nitrogen, and stored at −80°C. For reconstitution, the preformed liposomes were destabilized by the addition of 0.5% *n*-octyl-β-D-glucopyranoside (OG; Affymetrix). Purified EcClC was subsequently added at an initial concentration of 10 mg/ml. Depending on the lipid-to-protein ratio (LPR), 40, 16, or 8 µg of protein was added per milligram of lipids to obtain LPRs of 25, 63, and 125, respectively. The mixture was incubated for 5 min at 4°C and diluted 300 times into the reconstitution buffer. Proteoliposomes were collected by ultracentrifugation (60 min, 504,000 *g*) with a Type 70 Ti rotor (Beckman Coulter), then resuspended in 8 ml of reconstitution buffer followed by another ultracentrifugation step (60 min, 287,000 *g*) with an MLA-55 rotor (Beckman Coulter). The final resuspension volume was adjusted to obtain a lipid concentration of 5 mg/ml. The suspension containing EcClC-reconstituted liposomes was briefly sonicated, aliquoted, frozen in liquid nitrogen, and stored at −80°C.

Freeze-fracture and transmission electron microscopy

For quantification of the liposome size, samples were applied on a copper grid, flash-frozen in liquid ethane, and imaged on an electron microscope (TITAN Krios; FEI).

For freeze-fracture electron microscopy, liposomes were applied on a copper grid, sandwiched between specimen carriers, and frozen in a high-pressure freezing system (EM HPM100; Leica). Frozen samples were transferred to a freeze-fracturing device (BAF060; Leica) and fractured at −150°C. The fractured surfaces were coated with 2.5 nm of platinum/carbon by electron beam evaporation at an angle of 45°, and with 20 nm of carbon at an angle of 90°. Subsequently, replica were imaged with a transmission electron microscope (Philips CM 100; FEI) equipped with a charge-coupled device camera (Orius SC 1000; Gatan).

SSM measurements

SSM measurements were performed as described previously on a custom-built system (Schulz et al., 2008; for details see the supplemental tutorial file). In brief, a lipid monolayer was painted on a functionalized gold electrode forming the SSM electrode. The electrode was placed in the flow pathway of a flow-through cuvette. After thawing and gentle sonication, 40 µl of EcClC-reconstituted liposomes were added to the cuvette and allowed to adsorb to the electrode for 1 h. In a typical experiment, two solutions were used: a nonactivating solution depleted of chloride (containing 600 mM mannitol, 400 mM K_2SO_4, 100 mM potassium phosphate, and 25 mM citrate, pH 4.0) and an activating solution containing chloride (typically 300 mM KCl, 400 mM K_2SO_4, 100 mM potassium phosphate, and 25 mM citrate, pH 4.0). Sulfate was added to reduce the background currents due to nonspecific interactions of chloride with the lipid headgroups. For solutions containing lower chloride concentrations, KCl was replaced by twice the molar equivalents of mannitol to keep the osmolarity constant. For characterization of the pH dependence, the pH in activating and nonactivating solutions was adjusted with KOH, and pH was equilibrated before recording. The solution exchange protocol consisted of three phases: (1) the nonactivating solution flows for 2.5 s; (2) the activating solution flows for 2 s; (3) and the nonactivating solution flows for 2.5 s. Time in figures refers to the start of the flow of the activation solution. A valveless diverted fluidic geometry was chosen to apply the different solutions at a flow rate of 0.46 ml/s. pH-jump experiments were recorded with activating and nonactivating solutions containing 300 mM KCl, 400 mM K_2SO_4, 100 mM potassium phosphate, and 25 mM citrate. The respective pH was adjusted by addition of KOH. Background currents were recorded with solutions depleted of Cl^-. For inhibition experiments with 4,4′-diisothiocyano-2,2′-stilbenedisulfonic

acid (DIDS), the inhibitor-containing solution was freshly prepared by dissolving DIDS in nonactivating solution before the experiment.

Online supplemental material

Fig. S1 shows an analysis of the orientation of the protein in liposomes prepared by two different reconstitution methods. Fig. S2 displays an analysis of the liposome size by transmission electron microscopy and of the protein density by freeze-fracture electron microscopy. Fig. S3 demonstrates the stability of the SSM and shows recordings from proteoliposomes containing intracellular chloride. Fig. S4 shows the currents derived from a kinetic analysis assuming different transport rates. Fig. S5 displays the irreversible inhibition of EcClC by DIDS in proteoliposomes prepared by two different reconstitution methods. Fig. S6 addresses the leakiness of proteoliposomes for protons. Fig. S7 shows the lack of proton transport in the mutant E148A. A detailed tutorial describing the experimental setup and the measurement protocol of a SSM experiment is included as a PDF. Online supplemental material is available at http://www.jgp.org/cgi/content/full/jgp.201210927/DC1.

RESULTS

H^+/Cl^- antiport assayed by SSM electrophysiology

For recording of transport-mediated currents, proteoliposomes containing reconstituted EcClC were adsorbed on a SSM-coated gold electrode (sensor). Because of the strong interactions between the lipids of the vesicles and the lipid monolayer of the electrode, the proteoliposomes are essentially immobilized and the SSM thus forms a capacitively coupled system with high mechanical stability. The electrogenic exchange activity of EcClC was investigated upon rapid application of solutions containing chloride (activating solutions) after the incubation of the system with a chloride-free (nonactivating) solution, which we call a concentration jump. The establishment of a substrate concentration gradient creates a driving force for coupled electrogenic chloride/proton exchange, which can be recorded as an electrical current. Because the potential across the membrane evolves freely, the flow of ions generates an inside negative potential, which acts to decelerate the exchange reaction, thus leading to a decay of the current toward the baseline. Any net transport ceases at the reversal potential when the system has reached its equilibrium. The recorded currents are thus transient.

EcClC-mediated ion transport was measured from vesicles reconstituted at high protein concentrations (i.e., at a LPR of 25:1 wt/wt). Liposomes were prepared by extrusion through filters with a cutoff of 400 nm. The protein was incorporated after destabilization of the liposomes by addition of 0.5% of OG followed by the dilution of the sample to remove traces of the detergent. We have evidence that by our reconstitution method the proteins insert into the vesicles with a predominant inside-out orientation. This assumption is supported by experiments probing the accessibility of the C terminus from the outside of the vesicle: In liposomes obtained in the described way the tag is essentially quantitatively removed by proteolysis (Fig. S1), whereas ∼50% of the tags are inaccessible to proteolysis in samples prepared by reconstitution methods using detergent-solubilized lipids followed by the removal of the detergent by dialysis, which have previously been reported to result in a mixed orientation of the protein (Matulef and Maduke, 2005; Fig. S1). The quantification of the vesicle size by electron microscopy revealed a broad distribution of liposomes ranging between 60 and 240 nm with a maximum around 80 nm (Fig. S2 A). More than 90% of the vesicles were found to be unilamellar. The protein density within liposomes was determined by freeze-fracture electron microscopy (Fig. S2 B). Proteins are readily identified as knoblike protrusions, which are not found in empty liposomes. By analyzing the freeze fractures of 27 liposomes of different size, a mean protein density of 75 ± 15 EcClC dimers/μm^2 was obtained. Fig. 1 A shows the currents induced by a concentration jump with a solution containing 300 mM chloride. Measurements were performed at pH 4.0 on both sides of the membranes, a condition at which the transport activity of EcClC is high. As expected from the negative charge displacement during the 2:1 Cl^-/H^+ exchange reaction, the currents are negative, they rapidly increase after the exposure to chloride-containing solution, and they reach a maximum after ∼8 ms. The following decay is slower: after 20 ms the currents have returned to ∼90% of their maximum value, whereas the return to equilibrium is very slow and difficult to determine as the currents soon decay below the detection limit and vanish within the background of the recording. Under the described conditions, the peak current reaches about −16 nA. Because the adsorption of liposomes to the SSM was performed under saturating conditions, similar currents were obtained from independent measurements using vesicles from several reconstitutions of the protein (−15.4 ± 2.1 nA as determined from nine independent measurements). In contrast to the large transport-related signals, the background currents of empty liposomes recorded under the same conditions are small and positive (0.3 nA, Fig. 1 A). The mechanical stability of the coated SSM electrode is underlined by the fact that the amplitudes of currents obtained by the repeated application of concentration jumps followed by incubation with nonactivating solution are stable for hours, far beyond the measurement period (Fig. S3 A). The SSM is thus an ideal method to investigate the transport properties of EcClC from the same population of proteins under various conditions.

Although the recorded currents could in principle also originate from an electrogenic binding event where chloride ions cross part of the transmembrane electric field to occupy their binding sites, we assume that they reflect the transport of ions into the liposome. This assumption is sensible because, in a proteoliposome containing

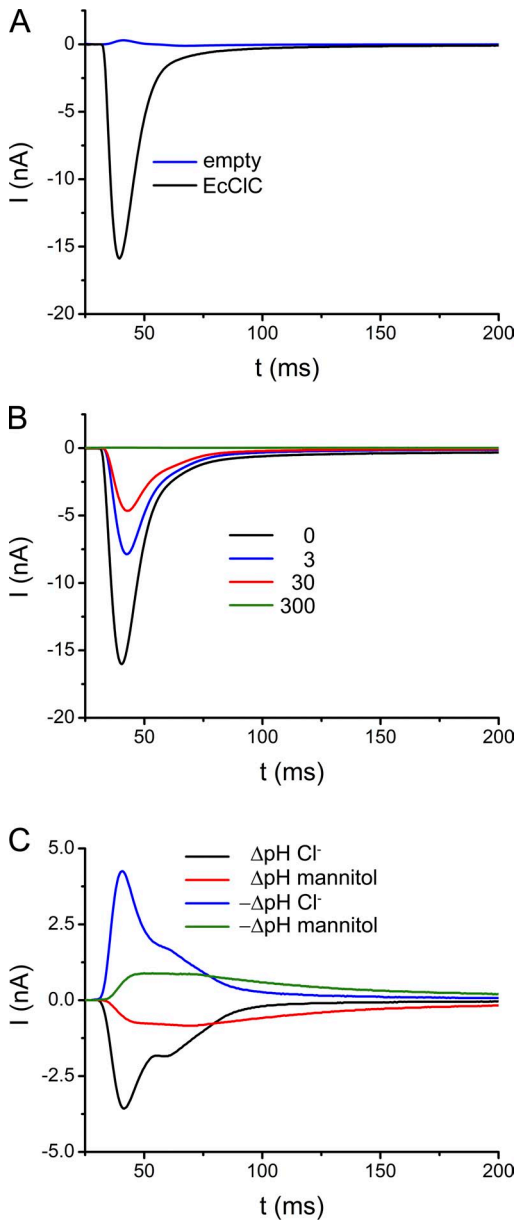

Figure 1. Transport-mediated currents in EcClC. (A) Transient currents recorded from EcClC containing proteoliposomes (LPR 25) in response to a 300 mM Cl^- concentration jump (applied at t = 0 after incubation with nonactivating solution containing 600 mM mannitol; black). Background from empty vesicles is shown in blue. (B) Transient currents recorded upon a concentration jump to 300 mM Cl^- after the equilibration of the vesicles with nonactivating solutions containing different Cl^- concentrations (0 mM, black; 3 mM, red; 30 mM, blue; 300 mM, green). To maintain osmotic balance, the concentration of mannitol of the nonactivating solution was decreased accordingly. Currents in A and B were recorded at pH 4.0. (C) Currents induced by an H^+ gradient. The traces were recorded upon pH jumps from pH 3.8 to 6.0 (black) and from pH 6.0 to 3.8 (blue). Activating and nonactivating solutions contained 300 mM Cl^-. Background currents induced by pH jumps were recorded from solutions where Cl^- was replaced by 600 mM mannitol.

75 dimeric transporters/μm^2 and an estimated intravesicular concentration of 30 µM, each subunit would undergo ~12 transport cycles in response to a 300 mM concentration jump before the equilibrium is reached (see Appendix). To further rule out the possibility that the observed currents reflect binding, we incubated our liposomes in solutions already containing chloride at sufficient concentrations to saturate ion binding sites in the protein (Picollo et al., 2009). In the case of a pure binding event, we would thus not expect to measure any currents upon a concentration jump to 300 mM. Fig. 1 B shows the transient currents recorded from vesicles incubated with nonactivating solutions containing either 3 or 30 mM chloride before activation. In this case, chloride binding sites accessible to the outside of the proteoliposome are occupied and a membrane potential corresponding to the respective chloride concentration is established. Fig. S2 B shows a similar experiment using proteins reconstituted into liposomes already containing 30 mM chloride, which saturates chloride binding sites accessible to both sides of the membrane but does not establish a membrane potential. Even in such cases a concentration jump induces sizable currents, although with smaller amplitude, which is expected from the decreased driving force caused by the transport against a preestablished membrane potential or a smaller concentration gradient. Because ion transport through EcClC couples the movement of Cl^- to the exchange of H^+, we also can use pH jumps to trigger transport. Such experiments are shown in Fig. 1 C, where a change in the proton concentration by 2.2 pH units induces measurable transport. However, because the change in the pH also causes transport-unrelated artifacts (probably due to the change of the protonation of bilayer lipids), measurements induced by concentration jumps of permeating anions are better suited for a quantitative interpretation.

A kinetic model of ion transport

The size and shape of the measured currents reflecting the electrogenic transport activity of EcClC is proportional to the turnover of a single transporter, the number of transporters per liposome, the number of EcClC-containing liposomes immobilized on the SSM electrode, and the total capacitance of the system (which depends on the combined surface of adsorbed liposomes, for details see Appendix). To better understand the underlying processes, we have simulated it with a model detailed in the Appendix of this manuscript. In this model the transport cycle is approximated by three steps describing the binding of ions from one side, a rate limiting electrogenic translocation step, and the dissociation of the ions on the opposite side. The model allows us to analyze the time course of the currents, their dependence on the reaction rates, and the evolution of the membrane potential during transport. By assuming rates comparable to the experimental conditions, this simulation reveals

a very similar evolution of currents with a fast increase leading to a maximum followed by a slow decay (Fig. 2 A). At the maximum, the membrane potential has only reached ~10% of its value at equilibrium (Fig. 2 A). After the current has decayed by 90%, the total amount of transported charge is still <50% (Fig. 2 B). The simulations thus show that the peak current is reached before a significant membrane potential is established, and they also underline the fact that it takes a long time to reach the equilibrium as the generated membrane potential progressively slows transport. These effects are even more pronounced if the reactions are slowed either by reducing the rate per transporter or by lowering the protein density (Fig. 2, A and B). In both cases the evolution of the signal is slower, the peaks are proportionally lower, and the time to reach equilibrium gets significantly prolonged. For example, when assuming a fivefold lower density of reconstituted transporters per vesicle, the currents reach their maximum, which is considerably lower than at higher protein density, later, and they decrease at lower membrane potential (5% of the equilibrium potential). Although the total charge transported to reach equilibrium only depends on the capacitance of the system and thus is the same independent of the transport kinetics, equilibration takes significantly longer for vesicles containing fewer transporters, and in the corresponding SSM traces it thus appears that less charge was moved (Fig. 2 A). The kinetics of transport are reflected in the initial slope of the recordings and the value of the peak currents. However, because the measurement of the initial slope for fast reactions is limited by the spread of the solution after a concentration jump over the area of the SSM and thus cannot be fully accessed in our experimental system, we chose the height of the peak current as measured for the transport rate. This assumption is justified in our simulations where the peak current is nearly proportional to the transport rate over a broad range of conditions in systems either containing fewer transporters or where the turnover per transporter was assumed to be lower (Fig. 2 C and Fig. S4). To probe whether we observe a similar relationship in our recordings, we have reconstituted EcClC at lower protein concentrations (i.e., LPR of 63:1 and 125:1 wt/wt) and have measured the electrogenic response upon application of a chloride concentration jump (Fig. 2 D). Similar to measurements at higher protein density (LPR 25), the obtained currents were also in these cases quantitatively reproduced in independent

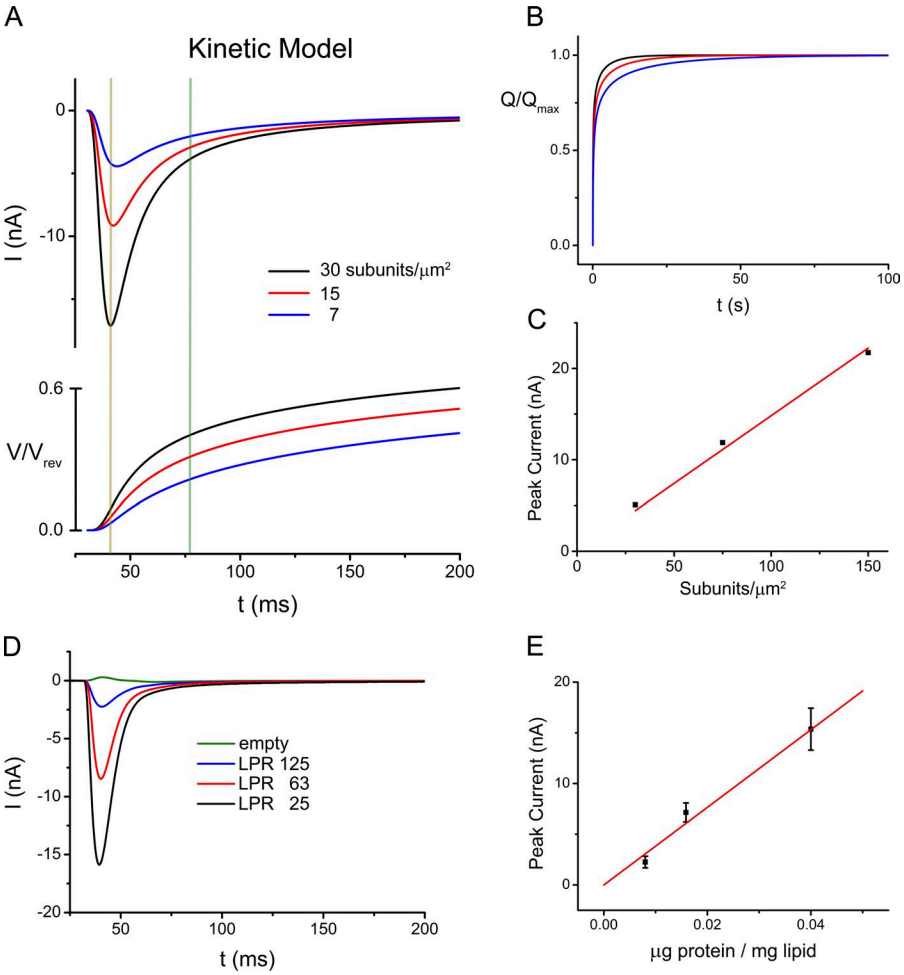

Figure 2. Kinetic modeling and transport at different LPRs. (A) Time dependence of currents obtained from a numerical simulation of a three-state kinetic model at different protein densities (top) and evolution of the membrane potential (bottom). The orange line indicates the position of the current maximum of vesicles with higher numbers of transporters. The green line indicates the position in the same recording where the current has decayed to 90% of its maximum. (B) Time-dependent accumulation of translocated charge obtained from the simulation shown in A. Colors in A and B correspond to different densities of transporters: black, 150; red, 75; blue, 30 subunits/µm^2. (C) Approximated linear relationship (red) between the simulated current maxima (I_{max}) and the number of transporters per liposome. (D) Transient currents measured from liposomes of proteins reconstituted at different LRPs. Currents were recorded at pH 4.0 in response to a 300 mM Cl^- concentration jump. (E) Approximated linear relationship (red) between recorded currents and the LPR. Data are averages of 4–9 independent measurements, errors bars indicate SEM.

experiments. As in the simulations, the peak heights in liposomes containing fewer transporters are lower, and we see a similar linear relationship between the current maxima and the reconstituted amounts of protein, thus suggesting that the approximation to use the peak heights to measure transport is also justified in our experimental systems (Fig. 2 E).

Anion selectivity and inhibition

ClC proteins are charge selective but they discriminate poorly between different monovalent anions. Because the peak heights in the recordings reflect the kinetics of ion transport, we can use the SSM method to directly compare the transport rates for different anions on the same sample. When replacing Cl^- with the equivalent concentrations of other monovalent ions such as Br^- or NO_3^-, which have previously been shown to be substrates of EcClC (Maduke et al., 1999; Nguitragool and Miller, 2006), we observed similar robust and reproducible currents as for Cl^-, although with reduced peak heights, which in the case of Br^- reach ~90% and for NO_3^- ~65% of the respective value of Cl^- (Fig. 3, A and B). In contrast to the weak discrimination between different larger monovalent anions, which are all efficiently transported with similar rates, the small halide ion fluoride is not a substrate for the transporter. In a concentration jump of F^- measured at pH 5, which is well above the pKa of hydrofluoric acid, no transport-related currents are observed (Fig. 3 C). Because the presence of equimolar amounts of F^- causes only a small decrease in the Cl^- currents, it can be assumed that F^- is essentially inert and does not strongly interact with the ion transport path of the protein (Fig. 3 D).

Next we have used the SSM method to study interaction of EcClC with the stilbenedisulfonate DIDS, which is known to irreversibly inhibit different anion channels and transporters by covalently binding to residues in the transport pathway (Jentsch et al., 2002) and which has previously been reported to affect the activity of EcClC (Matulef and Maduke, 2005).

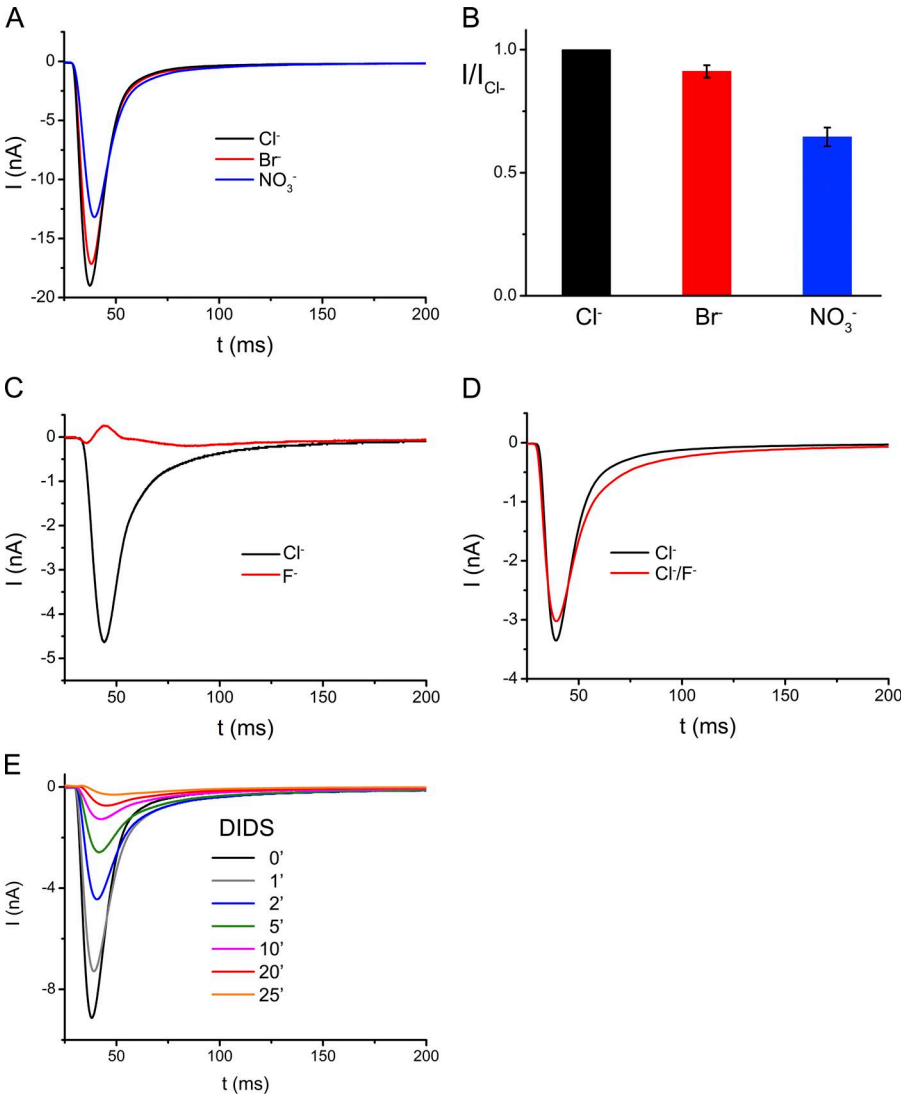

Figure 3. Ion selectivity and inhibition of EcClC. (A) Transient currents recorded from EcClC containing proteoliposomes at pH 4.0 in response to 300 mM concentration jumps of different transported anions. Data were recorded from the same sample. The traces in black, red, and blue correspond to currents induced by Cl^-, Br^-, and NO_3^-, respectively. (B) Relative transport rates of transported anions. Data shows averages of at least three independent experiments, errors bars indicate SEM. (C) Transient currents recorded from EcClC containing proteoliposomes at pH 5.0 in response to 300 mM concentration jumps of Cl^- (black) and F^- (red). Data were recorded from the same sample. (D) Transient currents recorded from EcClC containing proteoliposomes at pH 5.0 in response to application of solutions containing 150 mM Cl^- and 300 mM mannitol (black) and 150 mM Cl^- and 150 mM F^- (red). Data were recorded from the same sample. (E) Irreversible inhibition of EcClC by DIDS. The current response was measured after incubation of vesicles with 1 mM DIDS for different periods. Experiments were recorded at pH 4.0 from the same sample containing proteoliposomes with a preferred inside-out orientation of the transporter.

Upon incubation of vesicles adsorbed on the SSM with a solution containing 1 mM DIDS (at pH 4), a time-dependent irreversible decay of the current amplitude is observed. The current reaches about half of its maximum after 2 min and transport activity is essentially lost after 20 min (Fig. 3 E). Because the currents are quantitatively inhibited in samples with predominant inside-out orientation but only by ∼50% in liposomes containing proteins in both orientations, it can be assumed that DIDS irreversibly blocks the protein from the intracellular side (Fig. S5).

Chloride dependence of ion transport

The high mechanical stability of the SSM and the simple way to quantify the transport rates by measuring the maxima of the transient currents have allowed us to investigate the ion dependence of transport by applying substrate jumps at different Cl^- concentrations on the same set of transporters. To compensate for changes in the osmolarity of the solution, each equivalent of potassium chloride was replaced by twice the amount of mannitol. The data are displayed in Fig. 4 A. At low Cl^-, the transport rates strongly increase with concentration but the slope declines at higher concentrations, while the currents continue to increase even at 300 mM. A similar concentration dependence is observed for vesicles containing lower amounts of transport proteins, thus emphasizing that the observed effect reflects an intrinsic property of the reconstituted protein (Fig. 4 A). When fitted to a Hill equation, the data shows a half maximum transport rate at an ion concentration of 60 mM with a Hill coefficient of 0.6. The nonlinear concentration dependence of conduction and the negative cooperativity indicate multiple occupancy of binding sites and can be used for the comparison of mutants with altered transport properties.

pH dependence of ion transport

The transport through EcClC was previously shown to be strongly dependent on the proton concentration, with the protein being active at low pH and comparably inactive at higher pH (Lim and Miller, 2009). We were interested in determining the pH dependence of transport at conditions where the pH inside and outside the vesicle is equilibrated. A jump to 300 mM Cl^- thus creates the same driving force and any change of current peaks thus can be directly assigned to an altered transport rate. For equilibration we have, before the measurements, incubated the vesicles with solutions at the respective pH for an extended amount of time. For a titration, we have started the measurements at high pH and have subsequently decreased the pH by steps of 0.5–1 units. The extent of equilibration was probed by the measurement of transport-induced currents, which stabilized after an incubation time of ∼30 min (Fig. S6 A). Similar kinetics of equilibration were also observed in

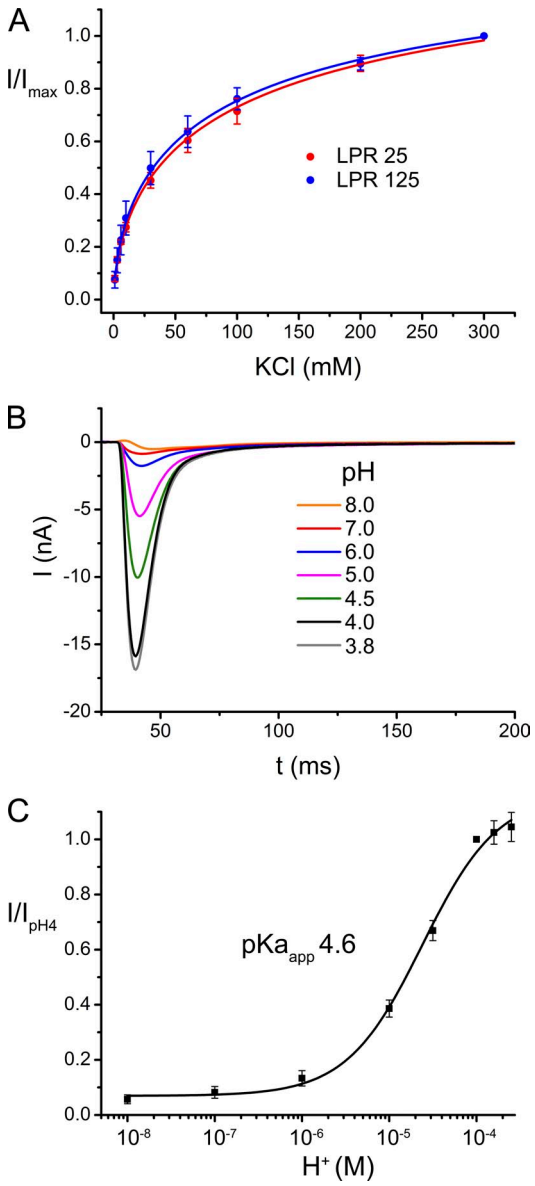

Figure 4. Concentration and pH dependence of EcClC. (A) Dependence of the peak currents on the chloride concentration for two different LPRs. Data for entire concentration range were recorded on the same sample at pH 4.0 upon application of solutions containing between 1 and 300 mM Cl^-. Mannitol was added to solutions to compensate for the decreased Cl^- concentration. Data were normalized to the current at 300 mM Cl^-. Averages of three independent experiments are shown, errors bars indicate SEM. (B) pH dependence of transport. Transient currents recorded upon application of 300 mM chloride concentration jumps at different pH values (between 8.0 and 3.8). For a given condition, the pH inside and outside the vesicle was equilibrated before measurements with activating and nonactivating solutions adjusted to the same pH value. Data were recorded from the same sample. (C) pH activation. Peak currents measured from one sample at different pH values were normalized to the data point at pH 4.0. Averages of 10 independent experiments are shown, errors bars indicate SEM. The solid line shows the fit to a single-site binding isotherm with an apparent pKa of 4.6.

a pH-sensitive fluorescence assay (Fig. S6 B), which suggests that the liposomes are leaky for protons over time, a behavior that was previously observed in other experiments (Mathai et al., 2001). A subsequent increase of the pH in SSM experiments followed by the return to acidic conditions resulted in very similar currents, thus excluding irreversible changes of the protein during the measurements. The pH dependence of transport could thus be measured over a broad range for the same set of vesicles and is shown in Fig. 4. The titration was reproduced several times for different samples with very similar results. Our data show that transport through EcClC is strongly pH dependent, with very low transport activity at pH 8.0 and maximal transport around pH 4.0. The data can be fitted to a single-site binding isotherm with an apparent pKa of 4.6, which is similar to the pKa of the carboxylate group of a glutamate side chain (i.e., 4.1–4.4).

Properties of mutants with altered transport behavior

To identify residues involved in the strong pH dependence of EcClC, we have investigated the effect of mutations of Glu_{ex} and Glu_{in} on the pH and chloride dependence of transport. In the mutant E148A, the side chain of Glu_{ex} was truncated. This mutant was previously shown to still conduct chloride but no longer to support coupled proton exchange (Accardi and Miller, 2004). In SSM experiments, this mutant does not mediate any currents in response to pH jumps that are larger than the background (Fig. S7), thus reinforcing the loss of proton conduction. The chloride dependence of transport in E148A shows measurable differences to WT. Despite a similar steep increase at low ion concentration, the following saturation is less pronounced and the concentration dependence is strong even at higher ion concentrations. Unlike WT, the mutant has lost its strong pH dependence and only shows a moderate, approximately linear decrease of transport at higher pH values with ∼60% of transport retained at pH 8.

The uncoupled mutant E203Q was also previously shown to have impaired H^+/Cl^- exchange, whereas it still conducts chloride (Accardi et al., 2005). Remarkably, the chloride concentration dependence of this mutant and WT are indistinguishable (Fig. 5 A). Transport by E203Q is still pH dependent with a maximum reached around pH 4.0, but unlike WT the mutant still shows considerable activity at high pH, which saturates at ∼25% of its maximum value above pH 6. When compared with WT, the apparent pKa of the mutant E203Q is slightly shifted by ∼0.3 units toward neutral pH. E203Q thus shows, despite its loss of coupled H^+ transport, a pronounced pH dependence and considerable activity even at high pH. Our results reinforce the finding that the side chain of Glu 148 is the main determinant for the pronounced pH dependence of EcClC, a result that is also underlined by the fact that the pH dependence in the double mutant E148A/E203Q is negligible (Fig. 5, D and E).

DISCUSSION

Our study has investigated the transport properties of EcClC, a bacterial H^+/Cl^- exchanger of the ClC family, by SSM electrophysiology. The rapid application of solutions containing transported anions to vesicles adsorbed to the SSM electrode triggers an electrogenic exchange reaction, which can be recorded as transient currents. Due to efficient reconstitution into the liposomes and the fast exchange kinetics of EcClC (with a unitary turnover of ∼2,000 s^{-1}; Walden et al., 2007), the currents are large and have allowed the detailed characterization of the process. By relating the recordings to a simple kinetic model, we have shown an approximately linear dependence of the transport rate to the maximum of the current response, which provides a simple method to compare the functional properties of the same population of molecules upon exposure to different environmental conditions.

The SSM method was previously used to study transport in the electrogenic transporters NhaA and LacY. Whereas, similar to EcClC, the turnover of the prokaryotic Na^+/H^+ exchanger NhaA is fast (i.e., 1,000 s^{-1}), and thus has allowed the recording of comparably large signals (Taglicht et al., 1991; Zuber et al., 2005), transport by the H^+/lactose symporter LacY is several orders of magnitude slower (i.e., 8 s^{-1}; Viitanen et al., 1984). Still, for both proteins (NhaA and LacY), the SSM-based experiments have provided the first characterization by electrophysiology (Zuber et al., 2005; Garcia-Celma et al., 2009, 2010), which underlines the potential of the method to investigate the functional properties even of slow transporters, whose transport-related currents are too small for classical electrophysiological experiments. Similar to EcClC, the turnovers of NhaH and LacY are strongly pH dependent, although with reversed direction, as the transporters are active at neutral pH whereas they are nearly inactive at low pH (Viitanen et al., 1983; Taglicht et al., 1991). This is remarkable, as transport in both proteins is coupled to H^+, and it underlines the fact that the pH dependence is an intrinsic property of the protein, which is used as regulatory mechanism in their physiological context (Iyer et al., 2002; Krulwich et al., 2011).

Our results on EcClC are in good agreement with data obtained from different biochemical and electrophysiological techniques, such as planar lipid bilayers, radioactive transport studies, and electrochemical measurements. In addition, the high mechanical stability of the SSM has facilitated the detailed characterization of anion selectivity, the concentration dependence of transported substrates, and the interaction with inhibitors on the same population of transporters. The investigation

of different substrates revealed similar transport rates for the related halide ions chloride and bromide and a somewhat lower rate for nitrate. These values are compatible with previous measurements, and they reinforce the weak selectivity of the transporter between different monovalent anions (Maduke et al., 1999; Accardi et al., 2004; Nguitragool and Miller, 2006). Plant ClC proteins show a stronger selectivity for nitrate where the anion is the main transported substrate (De Angeli et al., 2006). In contrast to larger anions, the small halide ion fluoride is not a substrate for EcClC, which may be related to the increased energy penalty for dehydration and the lack of suitable binding sites in the protein. It is thus remarkable that a branch of the ClC family has evolved as F^-/H^+ exchangers, which selectively transport fluoride but not chloride across membranes (Stockbridge et al., 2012). The measurement of relative transport rates upon application of different anions emphasizes the potential of the SSM method to characterize the substrate selectivity, which is particularly important for the investigation of novel transport proteins where this property is still unknown.

Our experiments also showed that DIDS, a known inhibitor of different chloride transport proteins, irreversibly inhibits transport in EcClC by accessing the ion translocation path from the intracellular side (Fig. 6). A similar, although reversible, inhibition by hydrolysis products of DIDS was previously reported from experiments in planar lipid bilayers (Matulef and Maduke, 2005). Although the source of the dissimilar behavior is not known it might be caused by differences in reaction conditions and the chemical instability of the molecule in solution (Matulef et al., 2008). The mode of sided irreversible inhibition of EcClC by DIDS resembles an equivalent process in the ion channel ClC-0 (Miller and White, 1980), and thus emphasizes the conserved structural properties of the family. The essentially complete inhibition also reinforces the preferred inside-out orientation of the protein in our samples. In contrast, the sample reconstituted by a different method, which is known to lead to a nonoriented distribution of the protein, shows only partial inhibition (Figs. S1 and S5).

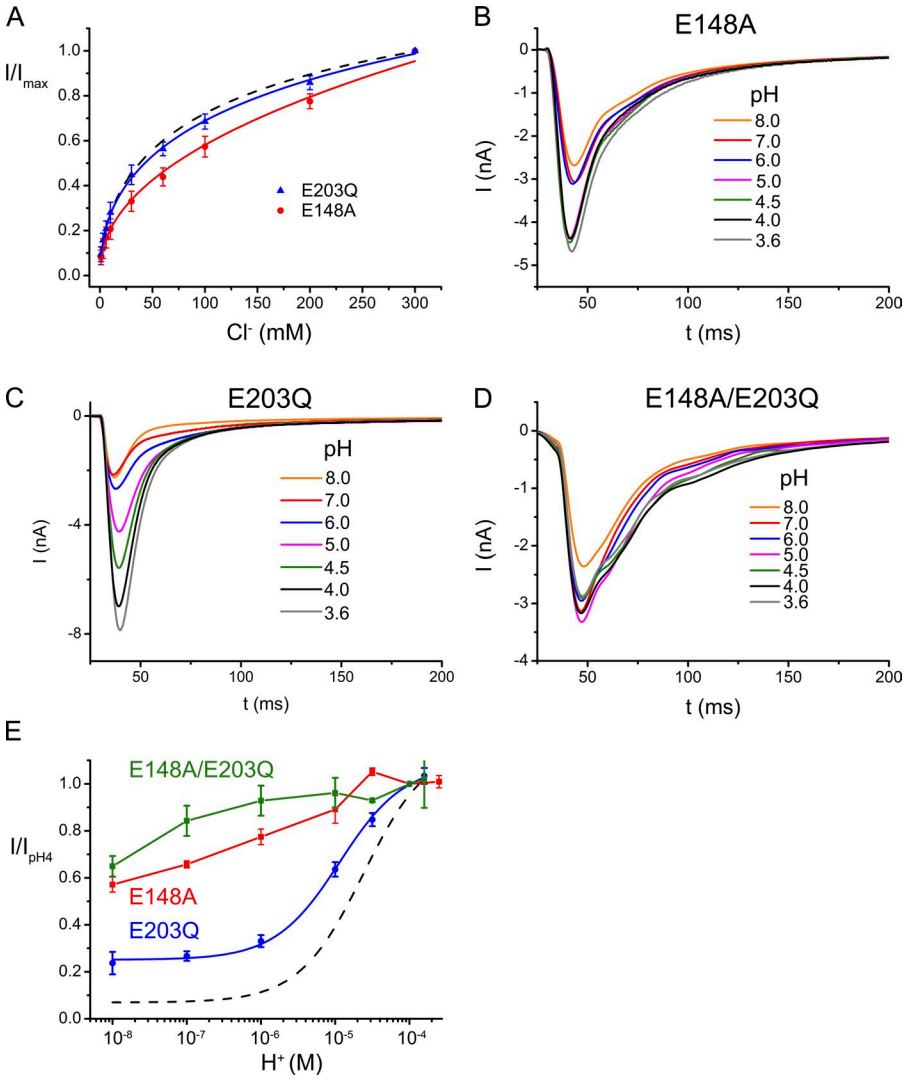

Figure 5. Concentration and pH dependence of EcClC mutants. (A) Cl^- concentration dependence of the point mutants E148A and E203Q were recorded as in Fig. 4 A. Data are averages of at least three independent measurements. Errors bars indicate SEM. WT is shown as a broken line for comparison. (B–D) pH dependence of mutants E148A (B) and E203Q (C), and the double mutant E148A/E203Q (D). Data were recorded as in Fig. 4 B. (E) Relative transport rates at different pH values normalized to pH 4.0 were obtained as in Fig. 4 C. Averages of at least three independent measurements are shown, error bars indicate SEM. Data points of the mutants E148A (red) and E148A/E203 (green) were connected by lines. The blue line shows a fit of the data of E203Q to a single site binding isotherm with an apparent pKa of 4.9 while allowing residual activity at low proton concentration. WT is shown as a broken line for comparison.

The SSM technique has allowed the characterization of the chloride dependence of transport, a property that, because of the difficulties in solution exchange, was not accessible to other techniques. Similar to other transmembrane transport proteins, the concentration dependence shows a Michaelis–Menten-like behavior, which probably reflects the occupation of ion binding sites. Although the mechanistic interpretation of the concentration dependence is not straightforward, it bears interesting resemblance to other experimental data. The negative cooperativity of the fit is compatible with the concurrent occupancy of closely spaced binding sites, which have been located in crystal structures of the protein, and the apparent K_M value of ∼60 mM matches the estimated affinity of a weak site at the intracellular entry of the ion-binding region (Lobet and Dutzler, 2006). It is also remarkable that a similar concentration dependence of the conductance was observed for the channels ClC-1 and ClC-0, thus underlining the conservation of the ion-binding properties within the ClC family (White and Miller, 1981; Rychkov et al., 1998).

Our measurements have allowed the quantification of the pH dependence of transport. EcClC is activated by protons; it reaches its maximum activity below pH 4.0 and is essentially inactive above pH 6.0. The apparent pKa of activation of 4.6 obtained from the SSM experiments is close to the value of the carboxylate side chain of glutamate residues, which were identified in EcClC as proton acceptors on both sides of the membrane. Proteins carrying mutations in either glutamate were previously shown to have lost the ability to catalyze coupled H^+/Cl^- exchange, whereas the proteins are still permeable to anions. One of the two residues, the extracellular Glu_{ex}, is the main determinant of the pronounced pH dependence, as its mutation to alanine renders transport nearly insensitive to changes in the proton concentration. The activity of a mutant of the intracellular acceptor Glu_{in} is still pH dependent, with a slight shift of the apparent pKa to less acidic values. In contrast to WT, in this mutant the transporter retains ∼25% of its activity at high pH, which indicates that here the chloride ion might be able to compete with the negatively charged side chain of Glu_{ex} for its binding site in the protein, thus opening the access of chloride ions to the extracellular side (Fig. 6 C). Our results are in accordance with previous measurements using an electrochemical chloride efflux method (Lim and Miller, 2009), but they deviate from a recent study that has characterized the pH dependence of transport from uptake assays and that proposed an apparent pKa that is shifted toward neutral conditions (Picollo et al., 2012).

The results of this study have established a robust system for the investigation of the activation and inhibition of EcClC in a wide range of conditions. The SSM thus complements the strengths of other assays of protein function and provides a powerful tool for the characterization of mutants with altered transport behavior. Although the transport mechanism in this important protein family is still controversial, it has become evident that it differs from established alternate access mechanisms found in other secondary active transport proteins (Accardi et al., 2006; Miller and Nguitragool, 2009; Feng et al., 2010, 2012). Additionally, some family members display complex regulatory properties in response to ligand binding that are currently not

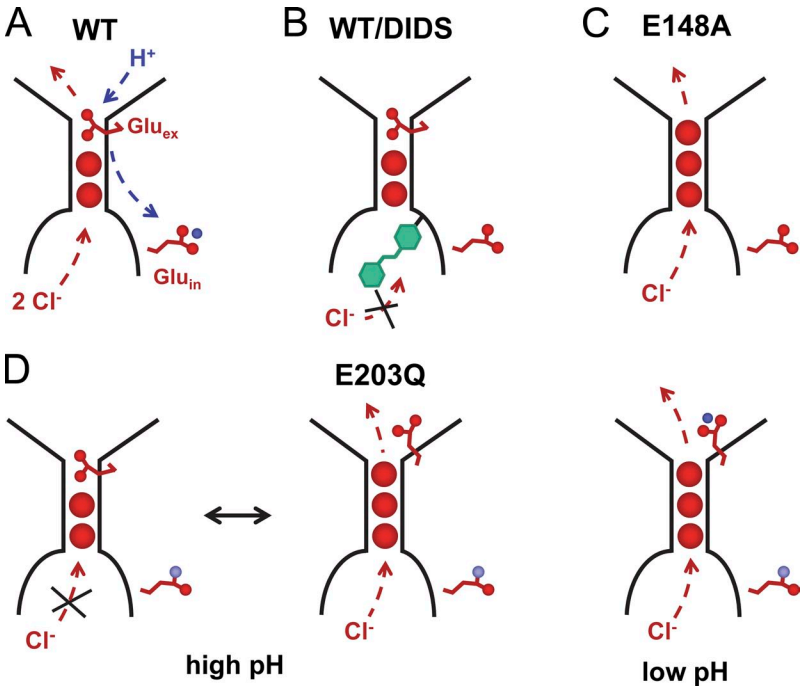

Figure 6. Transport phenotypes. Schematic depiction of the ion-binding region in EcClC. Bound Cl^- ions (red circles) and the side chains of two proton acceptors (Glu_{ex} and Glu_{in}) are shown. The direction of the transport during the SSM experiments is indicated by arrows. (A) WT. (B) EcClC inhibited by DIDS (green). (C) Mutant E148A. (D) Mutant E203Q at high (left) and low pH (right). At high pH, the negatively charged deprotonated Glu_{ex} competes with Cl^- for the same binding site, leading to partial activity of the protein. At low pH, the protonated Glu_{ex} is released from its binding site.

understood and for which the SSM method might provide a powerful tool (Meyer et al., 2007; De Angeli et al., 2009; Zifarelli and Pusch, 2009; Tseng et al., 2011). By revealing the relationship of the SSM data to observations by other experimental techniques, this study has also provided an important reference for future investigations of electrogenic transport proteins of currently unknown functions.

APPENDIX

For a better understanding of the signals observed in SSM experiments, this appendix estimates the number of transport cycles required to reach equilibrium, it discusses the three-step kinetic model used for the interpretation of the transient currents and approximates an analytical expression for the current maxima.

Charging of liposomes

In the described SSM experiments, the driving force for the inward flux of chloride in exchange with protons is generated by a rapid increase of the chloride concentration on the outside of the vesicle. The electrogenic exchange is accompanied by the buildup of a membrane potential (V), which counteracts transport. Any net flow of ions ceases at equilibrium, once the reversal potential (V_{rev}) of transport is reached. To estimate how many turnovers are needed to reach equilibrium, we assume that a minimal amount of chloride (c_{in} 0.03 mM) is kept inside the EcClC-reconstituted liposomes from previous chloride concentration jumps. Taking the transport stoichiometry of EcClC into account, the reversal potential for a 300 mM Cl^- concentration jump (c_{out}) can be calculated according to the following equation to be ∼−160 mV:

$$V_{rev} = -\left(\frac{1}{1+r}\right)\frac{RT}{zF} \times \ln\left(\frac{c_{in}}{c_{out}}\right).$$

For EcClC *r*, the stoichiometric ratio between the transported substrates is 0.5. z is the elementary charge of chloride, and R, T, and F describe the molar gas constant, the absolute temperature, and the Faraday constant, respectively. The charge (Q) per area that is moved across the liposome membrane to reach the reversal potential depends on the specific capacitance ($C_{specific}$ = 5.6 pF/μm^2) of a lipid bilayer. The number of turnovers ($N_{turnovers}$) per reconstituted protein that are needed to reach the reversal potential can thus be calculated according to the following equation, with e describing the elementary charge, q the net charge moved per transport cycle (i.e., 3), and ρ_{ClC} the density of transporters:

$$N_{turnovers} = \frac{V_{rev} \times C_{specific}}{e \times \rho_{ClC} \times q}.$$

For an LPR of 25:1, we have estimated ∼150 EcClC subunits/μm^2 (based on freeze-fracture electron microscopy; Fig. S2 B), whereas lower LPRs would contain proportionally less protein (i.e., 30 EcClC subunits/μm^2 for LPR 125). With this estimate, each subunit would undergo 12 transport cycles at LPR 25, and 60 cycles at LPR 125 before the thermodynamic equilibrium is reached.

A kinetic transport model

Because of the buildup of a membrane potential during transport, the turnover of the protein is not constant. The first transport cycles will take place at a much faster rate than later ones, where transported ions experience a significant inside negative potential. To simulate the time course of the transient currents and to estimate the time needed to reach equilibrium, a three-state kinetic model was constructed and solved numerically. For simplicity, the exchange of two chloride ions with one proton is represented as the translocation of one ion with three negative charges (χ^{3-}). The three partial reactions in the kinetic model were chosen as follows. The first partial reaction (A ↔ B) corresponds to the fast binding of χ^{3-} to the antiporter. The forward and backward rates for this step are 10^6 $M^{-1}s^{-1}$ and 3×10^4 s^{-1}, respectively. The second partial reaction (B ↔ C) represents the translocation of the ion through the membrane. This step is assumed to be electrogenic and rate limiting. The value of the forward and backward rate constants at zero membrane potential (k_2^0) is 1,000 s^{-1}, and their voltage dependence is assumed to follow Eyring rate theory. The third partial reaction (C ↔ A) represents the release of the ion from the antiporter. The forward and backward rates for this step are 3×10^4 s^{-1} and 10^6 $M^{-1}s^{-1}$, respectively. The model is, therefore, symmetrical.

Depending on the inside and outside chloride concentrations (c_{in} and c_{out}, respectively) and membrane potential (V_m), the rate constants are calculated as follows:

$$k_1^+ = c_{out} \times 10^6\, M^{-1}s^{-1}$$
$$k_1^- = 10^4\, s^{-1}$$
$$k_2^+ = k_2^0 \times \exp\left(-3 \times \frac{V_m}{2 \times RT/F}\right)$$
$$k_2^- = k_2^0 \times \exp\left(+3 \times \frac{V_m}{2 \times RT/F}\right)$$
$$k_3^+ = 10^4\, s^{-1}$$
$$k_3^- = c_{in} \times 10^6\, M^{-1}s^{-1}.$$

The current generated per transporter is calculated according the following equation, where e is the elementary charge,

$$I_{ClC}(t) = 3 \times e \times \left(k_2^+ \times B(t) - k_2^- \times C(t)\right).$$

Taking the capacitive coupling between the EcClC-reconstituted liposomes and the SSM into account and considering a nonconductive membrane, the electrogenic response of the antiporter is given by the following system of differential equations (Fendler et al., 1993):

$$\frac{dA(t)}{dt} = -k_1^+ \times A(t) + k_1^- \times B(t) - k_3^- \times A(t) + k_3^+ \times C(t)$$
$$\frac{dB(t)}{dt} = -k_1^- \times B(t) + k_1^+ \times A(t) - k_2^+ \times B(t) + k_2^- \times C(t)$$
$$\frac{dC(t)}{dt} = -k_3^+ \times C(t) + k_3^- \times A(t) - k_2^- \times C(t) + k_2^+ \times B(t)$$
$$\frac{dV_m(t)}{dt} = \frac{1}{Cm + Cp} N_{ClC} \times I_{ClC}(t),$$

where N_{ClC} is the number of antiporters per proteoliposome and C_p and C_m are the capacitances of a vesicle and the contact membrane, respectively. For simplicity, the same value was assumed for both capacitances. The system of differential equations is solved with the following initial conditions: $A(0) = 1$, $B(0) = C(0) = 0$.

The total current generated by all the proteoliposomes immobilized on the SSM is described by the following equation:

$$I_{SSM}(t) = C_m \times N_{Lip} \times \frac{dV_m(t)}{dt}.$$

Finally, to resemble the experimental conditions, the resulting currents have been convoluted with the transfer function corresponding to a concentration rise time of 8 ms (Garcia-Celma et al., 2008).

Analytical expression for the peak currents

To derive an analytical expression for the measured peak currents, the substrate concentration jump needs to be approximated by a step function. This approximation is supported by the result of the numerical simulation, which indicates that a negligible membrane potential is present at the time that the peak currents are reached. In this case, the peak current (I_{peak}) corresponds to the current measured at the initiation of the transport activity I_{SSM} [t = 0], which is related to the current generated by the transporter I_{ClC} [t = 0] by the following expression

$$I_{peak} \approx I_{SSM}\left[t = 0\right] = \frac{C_m}{C_m + C_p} \times N_{Lip} \times N_{ClC} \times I_{ClC}\left[t = 0\right].$$

Assuming that the reconstitution efficiency does not depend on the LPR, the peak currents are directly proportional to the amount of adsorbed EcClC-containing liposomes (N_{Lip}) and the amount of transporters incorporated per liposome (N_{ClC}). Indeed, we observed experimentally that the magnitude of the peak currents presents an almost linear dependence with the LPR of the immobilized liposomes. This relationship also highlights the correlation between the effect of the LPR and the turnover.

We thank Klaus Fendler for support during the establishment of the SSM setup and for fruitful discussions, Andres Käch and the Center for Microscopy and Image Analysis of the University of Zurich for help with freeze-fracture electron microscopy, Matthias Eibauer and Ohad Medalia for help with transmission electron microscopy, and Tina Schreier and all members of the Dutzler laboratory for help in all stages of the project.

The research leading to these results has received funding from a grant from the Swiss National Science Foundation (grant No. 31003B_141180) to R. Dutzler.

Christopher Miller served as editor.

Submitted: 2 November 2012
Accepted: 14 February 2013

REFERENCES

Accardi, A., and C. Miller. 2004. Secondary active transport mediated by a prokaryotic homologue of ClC Cl- channels. *Nature.* 427:803–807. http://dx.doi.org/10.1038/nature02314

Accardi, A., and A. Picollo. 2010. CLC channels and transporters: proteins with borderline personalities. *Biochim. Biophys. Acta.* 1798:1457–1464. http://dx.doi.org/10.1016/j.bbamem.2010.02.022

Accardi, A., L. Kolmakova-Partensky, C. Williams, and C. Miller. 2004. Ionic currents mediated by a prokaryotic homologue of CLC Cl- channels. *J. Gen. Physiol.* 123:109–119. http://dx.doi.org/10.1085/jgp.200308935

Accardi, A., M. Walden, W. Nguitragool, H. Jayaram, C. Williams, and C. Miller. 2005. Separate ion pathways in a Cl-/H+ exchanger. *J. Gen. Physiol.* 126:563–570. http://dx.doi.org/10.1085/jgp.200509417

Accardi, A., S. Lobet, C. Williams, C. Miller, and R. Dutzler. 2006. Synergism between halide binding and proton transport in a CLC-type exchanger. *J. Mol. Biol.* 362:691–699. http://dx.doi.org/10.1016/j.jmb.2006.07.081

De Angeli, A., D. Monachello, G. Ephritikhine, J.M. Frachisse, S. Thomine, F. Gambale, and H. Barbier-Brygoo. 2006. The nitrate/proton antiporter AtCLCa mediates nitrate accumulation in plant vacuoles. *Nature.* 442:939–942. http://dx.doi.org/10.1038/nature05013

De Angeli, A., O. Moran, S. Wege, S. Filleur, G. Ephritikhine, S. Thomine, H. Barbier-Brygoo, and F. Gambale. 2009. ATP binding to the C terminus of the *Arabidopsis thaliana* nitrate/proton antiporter, AtCLCa, regulates nitrate transport into plant vacuoles. *J. Biol. Chem.* 284:26526–26532. http://dx.doi.org/10.1074/jbc.M109.005132

Dutzler, R. 2007. A structural perspective on ClC channel and transporter function. *FEBS Lett.* 581:2839–2844. http://dx.doi.org/10.1016/j.febslet.2007.04.016

Dutzler, R., E.B. Campbell, M. Cadene, B.T. Chait, and R. MacKinnon. 2002. X-ray structure of a ClC chloride channel at 3.0 A reveals the molecular basis of anion selectivity. *Nature.* 415:287–294. http://dx.doi.org/10.1038/415287a

Dutzler, R., E.B. Campbell, and R. MacKinnon. 2003. Gating the selectivity filter in ClC chloride channels. *Science.* 300:108–112. http://dx.doi.org/10.1126/science.1082708

Fendler, K., S. Jaruschewski, A. Hobbs, W. Albers, and J.P. Froehlich. 1993. Pre-steady-state charge translocation in NaK-ATPase from

eel electric organ. *J. Gen. Physiol.* 102:631–666. http://dx.doi.org/10.1085/jgp.102.4.631

Feng, L., E.B. Campbell, Y. Hsiung, and R. MacKinnon. 2010. Structure of a eukaryotic CLC transporter defines an intermediate state in the transport cycle. *Science.* 330:635–641. http://dx.doi.org/10.1126/science.1195230

Feng, L., E.B. Campbell, and R. MacKinnon. 2012. Molecular mechanism of proton transport in CLC Cl-/H+ exchange transporters. *Proc. Natl. Acad. Sci. USA.* 109:11699–11704. http://dx.doi.org/10.1073/pnas.1205764109

Garcia-Celma, J.J., B. Dueck, M. Stein, M. Schlueter, K. Meyer-Lipp, G. Leblanc, and K. Fendler. 2008. Rapid activation of the melibiose permease MelB immobilized on a solid-supported membrane. *Langmuir.* 24:8119–8126. http://dx.doi.org/10.1021/la800428h

Garcia-Celma, J.J., I.N. Smirnova, H.R. Kaback, and K. Fendler. 2009. Electrophysiological characterization of LacY. *Proc. Natl. Acad. Sci. USA.* 106:7373–7378. http://dx.doi.org/10.1073/pnas.0902471106

Garcia-Celma, J.J., J. Ploch, I. Smirnova, H.R. Kaback, and K. Fendler. 2010. Delineating electrogenic reactions during lactose/H+ symport. *Biochemistry.* 49:6115–6121. http://dx.doi.org/10.1021/bi100492p

Graves, A.R., P.K. Curran, C.L. Smith, and J.A. Mindell. 2008. The Cl-/H+ antiporter ClC-7 is the primary chloride permeation pathway in lysosomes. *Nature.* 453:788–792. http://dx.doi.org/10.1038/nature06907

Iyer, R., T.M. Iverson, A. Accardi, and C. Miller. 2002. A biological role for prokaryotic ClC chloride channels. *Nature.* 419:715–718. http://dx.doi.org/10.1038/nature01000

Jayaram, H., J.L. Robertson, F. Wu, C. Williams, and C. Miller. 2011. Structure of a slow CLC Cl−/H+ antiporter from a cyanobacterium. *Biochemistry.* 50:788–794. http://dx.doi.org/10.1021/bi1019258

Jentsch, T.J. 2008. CLC chloride channels and transporters: from genes to protein structure, pathology and physiology. *Crit. Rev. Biochem. Mol. Biol.* 43:3–36. http://dx.doi.org/10.1080/10409230701829110

Jentsch, T.J., V. Stein, F. Weinreich, and A.A. Zdebik. 2002. Molecular structure and physiological function of chloride channels. *Physiol. Rev.* 82:503–568.

Krulwich, T.A., G. Sachs, and E. Padan. 2011. Molecular aspects of bacterial pH sensing and homeostasis. *Nat. Rev. Microbiol.* 9:330–343. http://dx.doi.org/10.1038/nrmicro2549

Lim, H.H., and C. Miller. 2009. Intracellular proton-transfer mutants in a CLC Cl-/H+ exchanger. *J. Gen. Physiol.* 133:131–138. http://dx.doi.org/10.1085/jgp.200810112

Lobet, S., and R. Dutzler. 2006. Ion-binding properties of the ClC chloride selectivity filter. *EMBO J.* 25:24–33. http://dx.doi.org/10.1038/sj.emboj.7600909

Maduke, M., D.J. Pheasant, and C. Miller. 1999. High-level expression, functional reconstitution, and quaternary structure of a prokaryotic ClC-type chloride channel. *J. Gen. Physiol.* 114:713–722. http://dx.doi.org/10.1085/jgp.114.5.713

Mathai, J.C., G.D. Sprott, and M.L. Zeidel. 2001. Molecular mechanisms of water and solute transport across archaebacterial lipid membranes. *J. Biol. Chem.* 276:27266–27271. http://dx.doi.org/10.1074/jbc.M103265200

Matulef, K., and M. Maduke. 2005. Side-dependent inhibition of a prokaryotic ClC by DIDS. *Biophys. J.* 89:1721–1730. http://dx.doi.org/10.1529/biophysj.105.066522

Matulef, K., A.E. Howery, L. Tan, W.R. Kobertz, J. Du Bois, and M. Maduke. 2008. Discovery of potent CLC chloride channel inhibitors. *ACS Chem. Biol.* 3:419–428. http://dx.doi.org/10.1021/cb800083a

Meyer, S., S. Savaresi, I.C. Forster, and R. Dutzler. 2007. Nucleotide recognition by the cytoplasmic domain of the human chloride transporter ClC-5. *Nat. Struct. Mol. Biol.* 14:60–67. http://dx.doi.org/10.1038/nsmb1188

Miller, C. 2006. ClC chloride channels viewed through a transporter lens. *Nature.* 440:484–489. http://dx.doi.org/10.1038/nature04713

Miller, C., and W. Nguitragool. 2009. A provisional transport mechanism for a chloride channel-type Cl-/H+ exchanger. *Philos. Trans. R. Soc. Lond. B Biol. Sci.* 364:175–180. http://dx.doi.org/10.1098/rstb.2008.0138

Miller, C., and M.M. White. 1980. A voltage-dependent chloride conductance channel from Torpedo electroplax membrane. *Ann. N. Y. Acad. Sci.* 341:534–551. http://dx.doi.org/10.1111/j.1749-6632.1980.tb47197.x

Nguitragool, W., and C. Miller. 2006. Uncoupling of a CLC Cl−/H+ exchange transporter by polyatomic anions. *J. Mol. Biol.* 362:682–690. http://dx.doi.org/10.1016/j.jmb.2006.07.006

Picollo, A., M. Malvezzi, J.C. Houtman, and A. Accardi. 2009. Basis of substrate binding and conservation of selectivity in the CLC family of channels and transporters. *Nat. Struct. Mol. Biol.* 16:1294–1301. http://dx.doi.org/10.1038/nsmb.1704

Picollo, A., Y. Xu, N. Johner, S. Bernèche, and A. Accardi. 2012. Synergistic substrate binding determines the stoichiometry of transport of a prokaryotic H(+)/Cl(-) exchanger. *Nat. Struct. Mol. Biol.* 19:525–531: S1. http://dx.doi.org/10.1038/nsmb.2277

Rychkov, G.Y., M. Pusch, M.L. Roberts, T.J. Jentsch, and A.H. Bretag. 1998. Permeation and block of the skeletal muscle chloride channel, ClC-1, by foreign anions. *J. Gen. Physiol.* 111:653–665. http://dx.doi.org/10.1085/jgp.111.5.653

Schulz, P., J.J. Garcia-Celma, and K. Fendler. 2008. SSM-based electrophysiology. *Methods.* 46:97–103. http://dx.doi.org/10.1016/j.ymeth.2008.07.002

Stockbridge, R.B., H.H. Lim, R. Otten, C. Williams, T. Shane, Z. Weinberg, and C. Miller. 2012. Fluoride resistance and transport by riboswitch-controlled CLC antiporters. *Proc. Natl. Acad. Sci. USA.* 109:15289–15294. http://dx.doi.org/10.1073/pnas.1210896109

Taglicht, D., E. Padan, and S. Schuldiner. 1991. Overproduction and purification of a functional Na+/H+ antiporter coded by nhaA (ant) from *Escherichia coli*. *J. Biol. Chem.* 266:11289–11294.

Tseng, P.Y., W.P. Yu, H.Y. Liu, X.D. Zhang, X. Zou, and T.Y. Chen. 2011. Binding of ATP to the CBS domains in the C-terminal region of CLC-1. *J. Gen. Physiol.* 137:357–368. http://dx.doi.org/10.1085/jgp.201010495

Viitanen, P., M.L. Garcia, D.L. Foster, G.J. Kaczorowski, and H.R. Kaback. 1983. Mechanism of lactose translocation in proteoliposomes reconstituted with lac carrier protein purified from *Escherichia coli*. 2. Deuterium solvent isotope effects. *Biochemistry.* 22:2531–2536. http://dx.doi.org/10.1021/bi00279a034

Viitanen, P., M.L. Garcia, and H.R. Kaback. 1984. Purified reconstituted lac carrier protein from *Escherichia coli* is fully functional. *Proc. Natl. Acad. Sci. USA.* 81:1629–1633. http://dx.doi.org/10.1073/pnas.81.6.1629

Walden, M., A. Accardi, F. Wu, C. Xu, C. Williams, and C. Miller. 2007. Uncoupling and turnover in a Cl−/H+ exchange transporter. *J. Gen. Physiol.* 129:317–329. http://dx.doi.org/10.1085/jgp.200709756

White, M.M., and C. Miller. 1981. Probes of the conduction process of a voltage-gated Cl- channel from Torpedo electroplax. *J. Gen. Physiol.* 78:1–18. http://dx.doi.org/10.1085/jgp.78.1.1

Zifarelli, G., and M. Pusch. 2007. CLC chloride channels and transporters: a biophysical and physiological perspective. *Rev. Physiol. Biochem. Pharmacol.* 158:23–76. http://dx.doi.org/10.1007/112_2006_0605

Zifarelli, G., and M. Pusch. 2009. Intracellular regulation of human ClC-5 by adenine nucleotides. *EMBO Rep.* 10:1111–1116. http://dx.doi.org/10.1038/embor.2009.159

Zuber, D., R. Krause, M. Venturi, E. Padan, E. Bamberg, and K. Fendler. 2005. Kinetics of charge translocation in the passive downhill uptake mode of the Na+/H+ antiporter NhaA of *Escherichia coli*. *Biochim. Biophys. Acta.* 1709:240–250. http://dx.doi.org/10.1016/j.bbabio.2005.07.009